

Development of Active Regions: Flows, Magnetic-Field Patterns and Bordering Effect

A.V. Getling¹ · R. Ishikawa² · A.A. Buchnev³

Received: 23 May 2015 / Accepted: 30 December 2015 / Published online: 12 January 2016
© Springer Science+Business Media Dordrecht 2016

Abstract A qualitative analysis is given of the data on the full magnetic and velocity vector fields in a growing sunspot group, recorded nearly simultaneously with the *Solar Optical Telescope* on the *Hinode* satellite. Observations of a young bipolar subregion developing within AR 11313 were carried out on 9–10 October 2011. Our aim was to form an idea about the consistency of the observed pattern with the well-known rising-tube model of the formation of bipolar active regions and sunspot groups. We find from our magnetograms that the distributions of the vertical [B_v] and the horizontal [B_h] component of the magnetic field over the area of the magnetic subregion are spatially well correlated; in contrast, the rise of a flux-tube loop would result in a qualitatively different pattern, with the maxima of the two magnetic-field components spatially separated: the vertical field would be the strongest where either spot emerges, while the maximum horizontal-field strengths would be reached in between them. A specific feature, which we call the *bordering effect*, is revealed: some local extrema of B_v are bordered with areas of locally enhanced B_h . This effect suggests a fountainlike spatial structure of the magnetic field near the B_v extrema, which is also hardly compatible with the emergence of a flux-tube loop. The vertical-velocity field in the area of the developing active subregion does not exhibit any upflow on the scale of the whole subregion, which should be related to the rising-tube process. Thus, our observational data can hardly be interpreted in the framework of the rising-tube model.

✉ A.V. Getling
A.Getling@mail.ru

R. Ishikawa
ryoko.ishikawa@nao.ac.jp

A.A. Buchnev
baa@ooi.sscs.ru

¹ Skobeltsyn Institute of Nuclear Physics, Lomonosov Moscow State University, Moscow 119991, Russia

² Hinode Science Center, National Astronomical Observatory of Japan, 2-21-1 Osawa, Mitaka, Tokyo 181-8588, Japan

³ Institute of Computational Mathematics and Mathematical Geophysics, Novosibirsk 630090, Russia

Keywords Velocity fields, photosphere · Magnetic fields · Active regions · Sunspots

1. Introduction

In the developing active regions (ARs), subphotospheric magnetic fields and fluid motions are strongly coupled according to the laws of magnetohydrodynamics. Obviously, the new magnetic flux emerges to the solar surface from deeper layers; if the emerging field is sufficiently strong, sunspot groups may develop. However, an intriguing issue related to this process is whether the strong magnetic field plays an active, primary role, having been formed in the depth of the convection zone and then emerging through the visible surface of the Sun, or the primary role is played by the fluid motion, which amplifies and structures the initially moderate or weak magnetic field.

The first of these alternatives is typically represented by the popular *rising-tube model* (RTM) according to which the magnetic field of a bipolar sunspot group originates from the emergence of an Ω -shaped loop of a coherent flux tube of strong magnetic field. As usually assumed, the flux tube forms in the general toroidal¹ solar magnetic field deep in the convection zone, and the field that this tube carries upward is already strong before the rise. This mechanism received much attention after a well-known study by Parker (1955), who invoked magnetic buoyancy to account for the rise of flux-tube loops. Later, the RTM has been revisited by a number of investigators over several decades. Interesting considerations of this model were suggested, in particular, by Caligari, Moreno-Insertis, and Schüssler (1995) and Caligari, Schüssler, and Moreno-Insertis (1998); numerical simulations of this mechanism based on full systems of MHD equations have also been carried out (see, *e.g.*, Fan, Featherstone, and Fang, 2013; Rempel and Cheung, 2014, and references therein).

The concept of RTM, which agrees with such important regularities of solar activity as Hale's polarity law and Spörer's law of sunspot-formation latitudes, appeared to be very attractive in the epoch of moderate capacities of observational instrumentation. For this reason, the idea of RTM remained virtually indisputable for a long time. Currently, the RTM still receives attention in both analyses of observational data and numerical simulations. In particular, under the assumption that a twisted flux tube (rope) rises in a developing AR, Luoni *et al.* (2011) and Poisson *et al.* (2015) estimate the magnetic helicity using the configurations of magnetic polarities in observed ARs.

However, some implications of the RTM were found to be hardly compatible with observations. In particular, if a flux-tube loop is rising, two very remarkable manifestations of this process should definitely be observed but, as we shall see, they do not conform with the observations discussed below:

- i) As the loop is rising, strong horizontal magnetic fields should emerge on the scale of the entire AR. It is the pattern of magnetic fields in a developing AR that will be the subject of our discussion here, and we shall find no manifestations of the loop rise.
- ii) Intense spreading from the site of the loop emergence should be observed over the whole AR. This is actually not the case; in particular, Pevtsov and Lamb (2006) "observed no consistent plasma flows at the future location of an active region before its emergence" and Kosovichev (2009) finds "no evidence for large-scale flows indicating future appearance [of] a large-scale magnetic structure". A further example of the horizontal-velocity

¹As frequently done in the literature on stellar and planetary dynamos, we use here the terms *toroidal* and *azimuthal* as synonyms, although they are not mathematically equivalent.

pattern without spreading on the scale of the whole developing AR is given by Getling, Ishikawa, and Buchnev (2015) (hereinafter, Paper I).

In addition, it is worth mentioning two other important considerations that are also not in favour of the RTM:

- iii) If the RTM is adopted, one has to account for the origin of the coherent tube of strong magnetic field deep in the convection zone. Various assumptions have been made to this end, which differ in their plausibility and the appropriateness of their starting points (see, e.g., a review by Fan, 2009, and references therein). Furthermore, before the emergence through the photospheric surface, such an intense flux tube should affect the structure of the convective velocity field, which is not actually observed, either.
- iv) Joy's law of the latitudinal dependence of the tilt angle of bipolar sunspot groups is not sensitive to the amount of the emerging magnetic flux in contrast to what could be expected: as Kosovichev and Stenflo (2008) and Kosovichev (2009) write, their "new statistical study of the variations of the tilt angle of bipolar magnetic regions during the flux emergence *questions the current paradigm* that the magnetic flux emerging on the solar surface represents large-scale magnetic-flux ropes (Ω -loops) rising from the bottom of the convection zone" (our italics).

These are the most important points of doubt about the universal applicability of the RTM; we shall not go here into further details, since we already discussed some of them in Paper I. In view of the contradictions of the RTM with observations and difficulties of accounting for the origin of the intense flux tube and some other features of the process, the rising-tube mechanism no longer appears to determine a paradigm in the studies of the development of ARs.

As alternatives to the RTM, various mechanisms of *in situ* magnetic-field amplification and structuring have been suggested. Among them, MHD mechanisms of inductive excitation of magnetic fields strongly coupled with fluid motions are usually referred to as *local dynamos*. This term is frequently used only in the context of small, granular scales and under; in contrast, we associate the concept of a local dynamo with a wider range of scales, including the sizes of the whole ARs (mesoscales).

The idea of local MHD dynamo traces back to Gurevich and Lebedinsky (1946), who related the amplification process to the effects of plasma motions; however, they did not attribute these motions to convection and even did not specify any particular type of motion. Tverskoi (1966) used a very simple model to demonstrate that the magnetic field can locally be amplified and structured by cellular magnetoconvection. Later, numerical simulations revealed the role of local dynamos as the producers of fairly disordered, intermittent magnetic fields on very small (down from the granular) scales (Cattaneo, 1999; Vögler and Schüssler, 2007; Kitiashvili *et al.*, 2015, etc.) In essence, only Stein and Nordlund (2012) used "realistic" numerical simulations to describe a convective mechanism capable of producing mesoscale amplified magnetic fields. They investigated the formation of an AR via the flux rise due to convective motions in the upper portion of the convection zone. The computed scenario does not imply the pre-existence of a coherent flux tube. A uniform, untwisted, horizontal magnetic field is initially present, and magnetic loops subsequently form over a wide range of scales. However, the initial field is required to be relatively strong, and only a moderate magnetic-field amplification (by a factor of about three) can be achieved. Previously, we discussed local convective dynamos in more detail (see Paper I).

Sunspot-formation mechanisms differing from a local dynamo were also suggested. Kitchatinov and Mazur (2000) investigated a hydromagnetic instability that can act on scales large compared to the granular size, producing a magnetic-flux concentration similar to those

Table 1 Summary of observational sessions.

Session No.	Date	Session meantime	Interval from (1)
1	09 Oct. 2011	19:31:15	00:00
2	10 Oct. 2011	01:06:16	05:35
3		06:30:15	10:59
4		15:00:14	19:29
5		21:46:15	26:15

observed in sunspots. The process crucially depends on the presence of fluid motion and on the quenching of eddy diffusivity by the enhanced magnetic field with the plasma cooling down. This is a local mechanism, which, however, is not a dynamo in the strict meaning of this term.

Another local mechanism, which does not qualify as a dynamo, is related to the so-called negative-effective-magnetic-pressure instability (NEMPI); see Warnecke *et al.* (2013, 2015) and references therein. It results from the suppression of the total turbulent pressure (the sum of hydrodynamic and magnetic components) by the magnetic field.

We present here a qualitative consideration of some observational data from the standpoint of items i) and ii) in the above list to decide whether or not these data can be interpreted in terms of the RTM. To obtain relevant data, we developed an observational program of studying the evolution of both the velocity and the magnetic fields in growing ARs. This program (operation plan) was intended for implementation with the *Solar Optical Telescope* (SOT) on the *Hinode* spacecraft (Tsuneta *et al.*, 2008; Suematsu *et al.*, 2008; Shimizu *et al.*, 2008) and has been designated as HOP181 (http://www.isas.jaxa.jp/home/solar/hinode_op/hop.php?hop=0181). It is aimed at simultaneously recording and analysing the dynamics of the full-vector velocity and magnetic fields on the photospheric level. Previously, we presented some preliminary results of our study (Paper I). New features of the AR evolutionary pattern inferred from our data will be given here.

2. Observations and Data Processing

A bipolar magnetic structure, which emerged within AR 11313, was observed at its early evolutionary stage, on 9–10 October 2011; the AR was then near the centre of the solar disc. Five 2-h-long observational sessions were carried out with intervals that varied from 3 h 40 min to 6 h 30 min (see the summary in Table 1).

During each session, a $150'' \times 163''$ field of view (FOV) was observed using the *Narrowband Filter Imager* (NFI) of the SOT at two wavelength positions of FeI λ 5776 Å with a time cadence of 2 min and a pixel size of $0.16''$. This yielded a series of photospheric images, which can be used to calculate horizontal² velocities [u_h], and a series of Dopplergrams representing the line-of-sight (LOS), or vertical, velocities [u_v]. Simultaneously, the same FOV was scanned with the *Spectro-Polarimeter* (SP; see Ichimoto *et al.*, 2008; Lites *et al.*, 2013) one or two times a session. The SP scan was done in the so-called fast mode

²Since the area of interest was located near the solar-disc centre and, moreover, corrections for projection effects are not important from the standpoint of our goal, we do not make difference here between the line-of-sight and the vertical component and also between the transversal (tangential) and horizontal vector components.

with a pixel size of $0.32''$, taking 32 min to obtain one SP map. To derive full-vector magnetic fields from these SP observations, we used the MERLIN inversion code (Lites *et al.*, 2007), which assumed a Milne–Eddington atmosphere.

The processing of the data included:

- i) Subsonic filtering based on a Fast Fourier Transform.
- ii) Constructing Dopplergrams.
- iii) An intensity-scaling procedure enhancing the image contrast by means of cutting off the tails of a pixel-intensity histogram and subsequent linear mapping of the remaining portion of the histogram onto the whole admissible intensity range.
- iv) Alignment of the magnetograms corrected for irregularities of the SP scanning process, with the properly rescaled images and Dopplergrams obtained at the mean time of the scan (the correction was done by choosing 30 or more reference points, typically pores or easily identifiable fine details of spots, in both the FG image and the image accompanying the magnetogram, and subsequently bringing them into coincidence by means of affine transformations).
- v) Determination of the horizontal-velocity field using a technique based on the same principle as the standard method of local correlation tracking (LCT) but more reliable (see Getling and Buchnev, 2010, for a description) and construction of cork-trajectory maps. Our technique differs from the standard LCT procedure in a special choice of trial areas (“targets”), whose displacements are determined by maximizing the correlation between the original and various shifted positions of the target. Specifically, an area is chosen as a target in a certain neighbourhood of each node of a predefined grid if either the contrast or the entropy of the brightness distribution reaches its maximum in this area. The horizontal velocities obtained are then interpolated to the positions of imaginary “corks” using the Delaunay triangulation and affine transformations specified by the deformation of the obtained triangles at the time step considered.
- vi) Elimination of the Sun’s rotation from the fields of LOS velocities.
- vii) Reducing the mean LOS velocity to zero in each map.

The MERLIN code yields the magnitude, inclination and azimuth of the magnetic-field vector (in parallel with a continuum image), which we then convert into the LOS and tangential components. In addition to the original maps of the vertical velocity and magnetic-field components, we used smoothed maps of these quantities.

3. Results

3.1. Evolution in White Light

The photospheric images of AR 11313 obtained during the five observational sessions are shown in Figure 1. They cover a time interval somewhat exceeding one day (see Table 1). It can be seen that a bipolar sunspot group has already formed by the first observational session. At nearly the same time, a new, minor sunspot group starts developing between the main spots of the previously developed group, in the left half of the FOV. This process becomes mainly accomplished by the third session, after which the spots of the newly born group continue growing and its leading and trailing spots move apart.

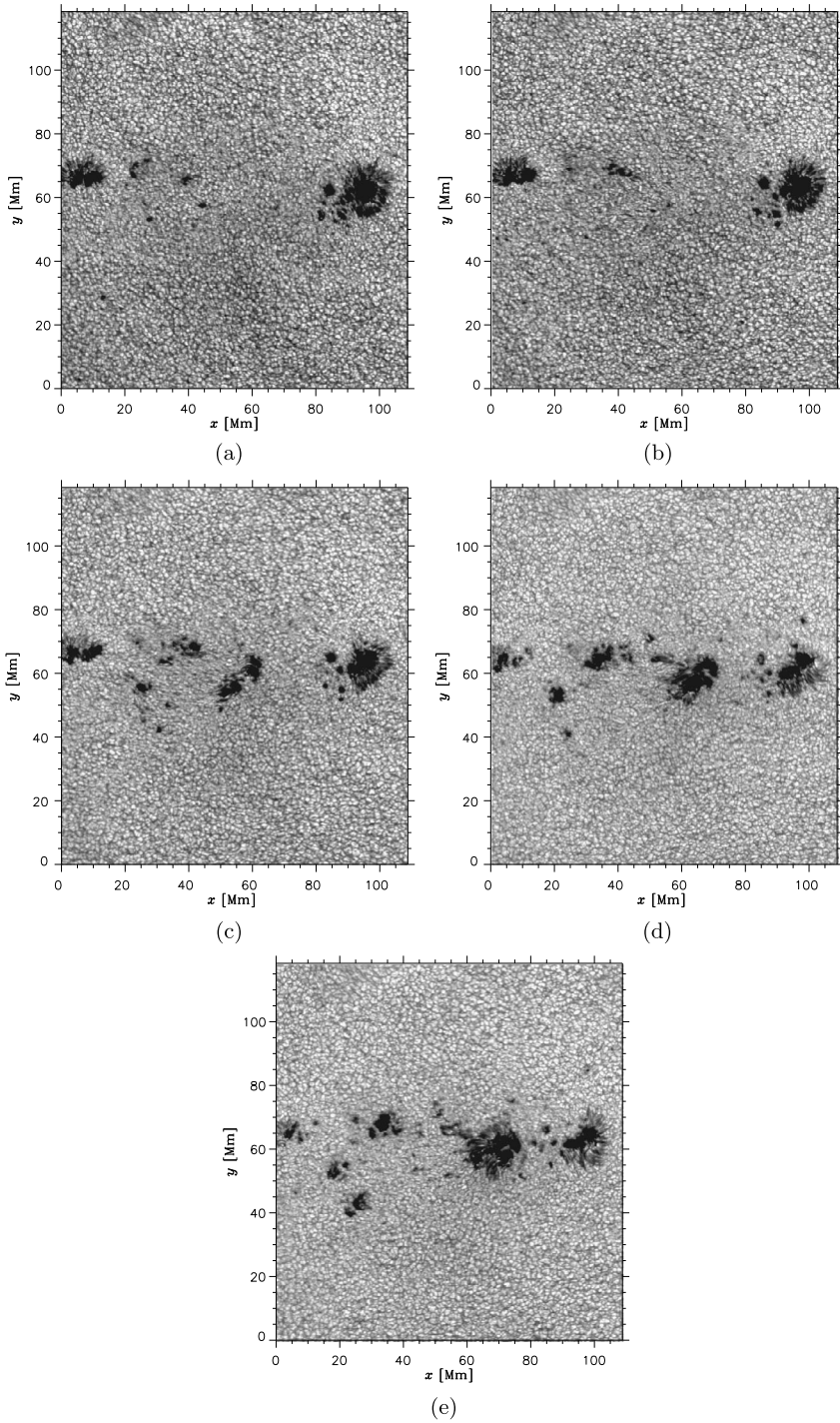


Figure 1 Evolution of AR 11313 in visible light. Images (a)–(e) were taken at the mean times of observational sessions (1)–(5) (see Table 1) with the SOT/NFI.

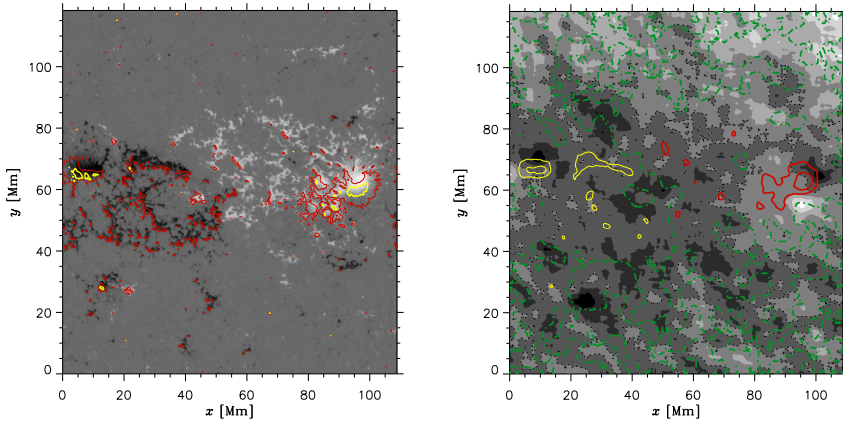


Figure 2 Left: comparison between the vertical (grey-scale map) and horizontal (contours) components of the magnetic field for observational session (1); the B_v range is $[-1941 \text{ G}, 2477 \text{ G}]$; contour levels for B_h are 800 G (red) and 1400 G (yellow). Right: comparison between the patterns of the smoothed vertical-velocity field (grey-scale filled contour map with the dotted contours for zero velocity) and smoothed vertical magnetic field (colour contours) for the same session; the contour increment is 800 G for magnetic field and 0.2 km s^{-1} for velocity; red contours correspond to $B_v > 0$, green dot-dashed contours to $B_v = 0$ and yellow contours to $B_v < 0$; the size of the smoothing window is 3.5 Mm for magnetic field and 7.4 Mm for velocity. The dark areas in both grey-scale maps correspond to negative values (vectors directed upward) and light areas to positive values (vectors directed downward).

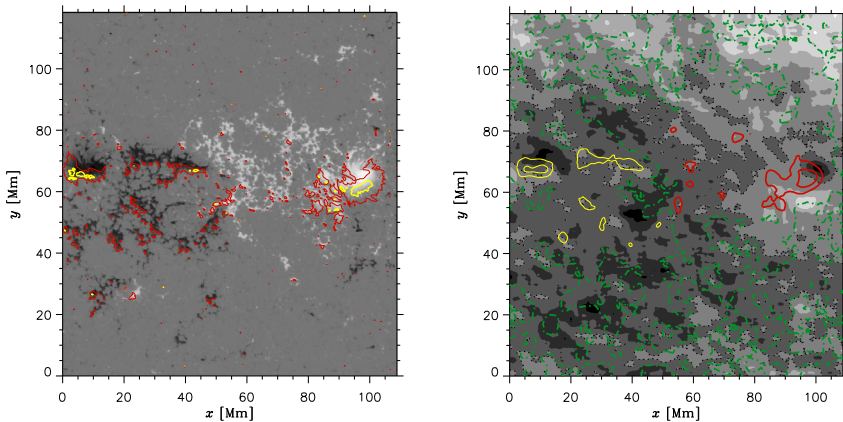


Figure 3 Same as in Figure 2 but for session (2); the B_v range is $[-2121 \text{ G}, 2460 \text{ G}]$.

3.2. Magnetic-Field Patterns. Bordering Effect

We consider here some features of the developing magnetic and velocity fields deducible from Figures 2–6, which refer to sessions (1)–(5), respectively. The left-hand panel of each figure makes it possible to compare the original (detailed) maps of the vertical [B_v] and horizontal [B_h] components of the magnetic field. As for confronting the vertical magnetic and velocity fields, a specific noise of fine details in the original maps makes comparisons between them difficult. In view of this, we use smoothed magnetic and velocity fields for such comparisons (right-hand panels).

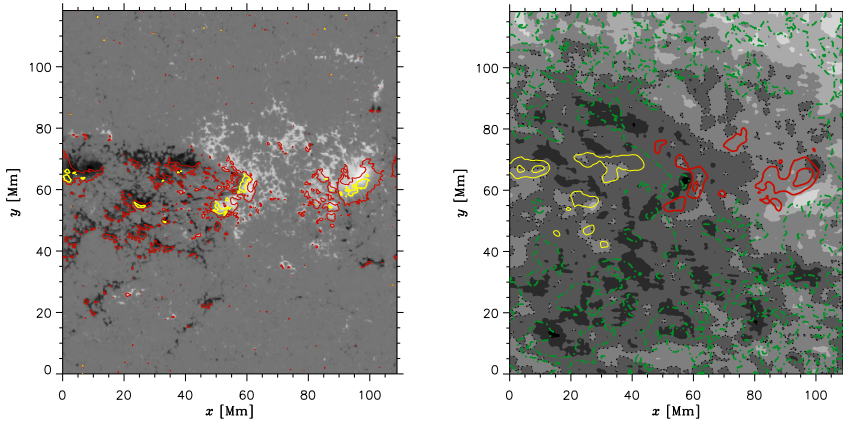


Figure 4 Same as in Figure 2 but for session (3); the B_V range is $[-2112 \text{ G}, 2467 \text{ G}]$.

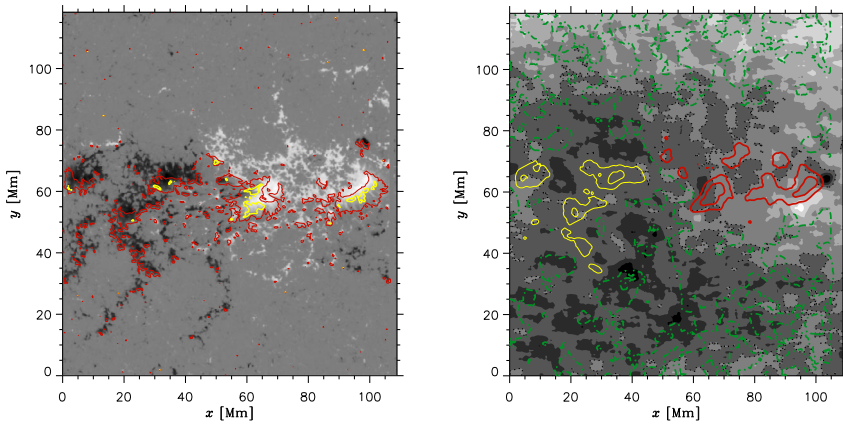


Figure 5 Same as in Figure 2 but for session (4); the B_V range is $[-2177 \text{ G}, 2217 \text{ G}]$.

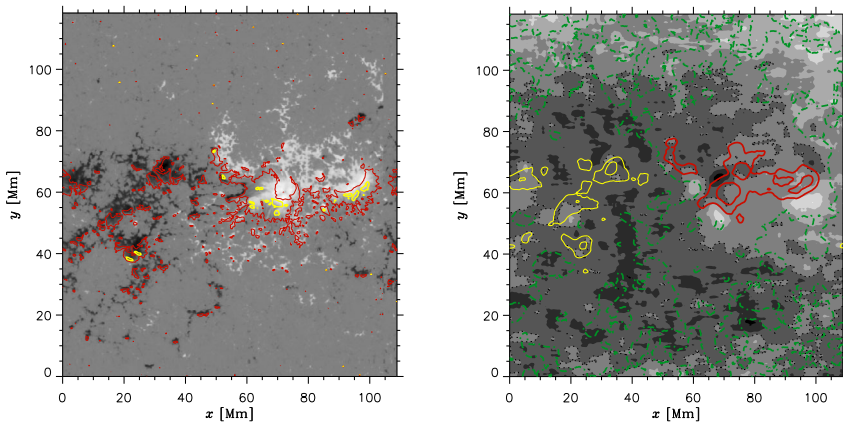


Figure 6 Same as in Figure 2 but for session (5); the B_V range is $[-2362 \text{ G}, 2316 \text{ G}]$.

Let us first note a remarkable feature of the magnetic field, which we call the *bordering effect*. It can be revealed in the magnetograms of all the five sessions by examining the left-hand panels but is most pronounced in Figures 5 and 6. While most local (mainly positive) extrema of B_v spatially coincide with areas of low B_h , these areas are partially bordered with arched areas of locally enhanced B_h .

The bordering effect admits a quite straightforward interpretation. Assume that magnetic field lines form a bundle issuing from the subphotospheric layers and diverge in its top section like the water jets in a fountain. In this case, B_v will obviously reach its peak magnitudes in the central part of the bundle, while B_h will be maximum in an annulus surrounding the bundle.

A common feature of all the magnetograms is fairly good, visually noticeable spatial correlation between the distributions of B_v and B_h (see left-hand panels in Figures 2–6). However, for a given sign of B_v , its pattern typically exhibits a relatively uniform spatial shift with respect to the corresponding, similar pattern of B_h (the contour representation of B_h clearly visualises this shift only in the areas of $B_v < 0$). The shifts for the two signs may differ in their magnitude and direction; they do not exceed 2 Mm.

The shift of the B_h pattern relative to the B_v pattern may be indicative of a systematic increase in the tilt of the magnetic field lines in the direction of this shift. This feature thus proves to be akin, in a sense, to the bordering effect, being a manifestation of the three-dimensional structure of the magnetic field.

To make further inferences from the magnetograms, we have to remember a feature that should be expected in the case of the flux-tube rise and was mentioned above as item i) in the list of RTM doubtful points (see the Introduction). Specifically, strong horizontal fields should connect the emergence areas of the main spots, forming elongated features where the horizontal-field strength values are comparable with the vertical-field strengths observed in the spots.

As for our magnetograms, they display signatures of finely structured horizontal field in the form of very narrow elongated features stretching between the main magnetic poles. These features are present in the obtained B_h distributions for sessions 3, 4 and (in a very faint appearance) 5 but can hardly be distinguished in their contour representations in the respective figures. In this context, the following should be noted. First, these features became noticeable after the formation of the bipolar configuration of strong magnetic field but were completely absent at the stage of development of this configuration. In contrast, if a flux-tube loop rose, we would see stretched features (not necessarily finely structured) earlier, during the sunspot-group development. Second, as the magnetograms demonstrate, the horizontal field in these features is considerably weaker (a factor of two to three) than the peak B_h values, which, in turn, do not exceed the peak values of B_v (see Table 2). Therefore, the scenario of magnetic-field development is not consistent with the RTM-based expectation indicated as item i) in the list of RTM doubtful points (see Introduction).

3.3. The Magnetic vs. the Velocity Field

Now let us compare the smoothed B_v and u_v fields shown in the right-hand panels of Figures 2–6 and discuss the relationship between them. It can be seen from our velocity maps that no marked upflow can definitely be related to the entire area where the rise of a flux-tube loop should be expected according to the RTM. In Figure 2, several moderate, localised upflows are present in this area, while the strongest upflows are present not far from the lower left corner of the FOV and near the existing sunspots. In Figure 3, an upflow-velocity maximum is located below the area of interest, being comparable in its magnitude with several

Table 2 Characteristic values of B_v and B_h in the developing AR.

Session No.	B_v range [G]	B_h range [G]	Typical B_h values in fine features [G]
1	(-1900)–2500	0–1900	800–1200
2	(-2100)–2500	0–1800	600–1000
3	(-2100)–2500	0–2100	700–1100
4	(-2200)–2200	0–1800	700–1100
5	(-2400)–2300	0–2200	600–1100

other local maxima. Nothing similar to a strong upflow associated with the hypothetical rising tube can be seen in Figure 4; see also Figures 5 and 6.

It is also worth remembering that the u_h field that we constructed based on the same observations as those discussed here (see Paper I) exhibits neither spreading flows on the scale of the whole developing group nor flows that are qualitatively different from normal mesogranular and supergranular convection unaffected by any large-scale disturbances.

Thus, the observed patterns of both the vertical and the horizontal velocity in the developing active subregion are at variance with the RTM-based expectation mentioned above as item ii) in the list of RTM doubtful points (see Introduction).

It is also interesting to note the following particular feature of the u_v field in the vicinity of the leading (rightmost) spot of the large group that was formed before the smaller group started developing. If we compare Figure 1a–c with B_v and u_v distributions in the right-hand panels of Figures 2–4, we can find that on two sides of the leading spot there are an upflow (above the spot in the FOV) and a downflow area (below it). This feature can also be distinguished (although is much less pronounced) in Figures 5 and 6.

4. Discussion and Conclusion

Our analysis of the observational data for the development of the minor subregion within AR 11313 on 9–10 October 2011 reveals a noticeable discrepancy between the observed development pattern of the magnetic and velocity fields and the RTM-based expectations.

First, we have found that the distributions of B_v and B_h over the area of the growing magnetic subregion are spatially well correlated, with a shift between the entire patterns of B_v and B_h by a distance of no larger than about 2 Mm. The rise of a flux-tube loop should result in a qualitatively different pattern. The maxima of the two magnetic-field components would be spatially separated in this case: the vertical field would be the strongest where either of the main spots emerges, with the maximum horizontal-field strengths reached in between them. Moreover, the horizontal field would form elongated features connecting the main spots, being comparable with the vertical-field strengths in these spots. In contrast, we observe finely structured elongated features, which emerged no earlier than the bipolar configuration of strong magnetic field had completely formed and were considerably weaker than the vertical field in the spots.

The feature that we call the bordering effect provides additional evidence against the rise of a tube, since it demonstrates a fountainlike three-dimensional structure of individual local magnetic-field maxima. It becomes pronounced by the final formation stage of the active subregion under study (Figure 4). Such a structure is hardly compatible with the emergence of a whole tube loop, which should produce local maxima of the vertical magnetic field only at the feet of the loop.

Second, the flow pattern observed in the area of the developing active subregion is not consistent with the idea of the flux-tube-loop emergence. There is no upflow on the scale of the whole subregion, which should be related to the rising-tube process. In addition, the horizontal-velocity field (considered in Paper I) does not exhibit any spreading flow on the scale of the entire growing magnetic region; instead, some motions resembling normal mesogranular and supergranular flows appear to be preserved. In this context, it is worth noting that, many years ago, Bumba (1963, 1967) and Bumba and Howard (1965) found that the growing magnetic fields do not break down the pre-existing convective-velocity field but come from below “seeping” through the network of convection cells. The development of a sunspot group seems to be controlled by the supergranular network, and the lines of force of the strong local magnetic fields are nearly collinear with the streamlines of the photospheric plasma. This can naturally be understood if the magnetic field is assumed to be formed by convective motions.

Thus, our observational data can hardly be interpreted in the framework of the rising-tube model. However, our inferences are based on a single AR-emergence event, which is insufficient to assess how typical the observed scenario is.

The emergence of 41 AR is analysed by Poisson *et al.* (2015) based on observations of the vertical magnetic fields. They use a model of the twisted flux tube (rope) to describe the time variations in the twist (and, accordingly, in the magnetic helicity). However, as can be observed, the assumption of the flux-tube rise is the starting point of their investigation and its results are discussed in comparisons with numerical simulations of the rising tubes. Since no possibilities lying beyond the framework of this concept are considered, it is not obvious that such alternatives should be ruled out in the cases considered.

The issue of the comparative role of different really possible active-region generation mechanisms thus remains open, and further observations are needed. In our view, they would be most promising if they include recording both magnetic and velocity fields. We plan such observations for the near future. Since the rising-tube mechanism does not appear to be universal, a local convective dynamo as the producer of the magnetic fields of active regions deserves close attention (see Paper I for a discussion of the relevance of this mechanism).

Acknowledgements *Hinode* is a Japanese mission developed and launched by ISAS/JAXA, with NAOJ as domestic partner and NASA and STFC (UK) as international partners. It is operated by these agencies in cooperation with ESA and NSC (Norway). The work of A.V.G. and A.A.B. was supported by the Russian Foundation for Basic Research (project no. 12-02-00792-a). We are grateful to L.M. Alekseeva and to the reviewer for their comments.

References

- Bumba, V.: 1963, Relation between motions and local magnetic fields in the photosphere. *Bull. Astron. Inst. Czechoslov.* **14**, 1. [ADS](#).
- Bumba, V.: 1967, Observations of solar magnetic and velocity fields. In: *Rendiconti della Scuola Internazionale di Fisica “E. Fermi”, 39 Corso*, 77.
- Bumba, V., Howard, R.: 1965, A study of the development of active regions on the Sun. *Astrophys. J.* **141**, 1492. [DOI](#). [ADS](#).
- Caligari, P., Moreno-Insertis, F., Schüssler, M.: 1995, Emerging flux tubes in the solar convection zone. I. Asymmetry, tilt, and emergence latitude. *Astrophys. J.* **441**, 886. [DOI](#). [ADS](#).
- Caligari, P., Schüssler, M., Moreno-Insertis, F.: 1998, Emerging flux tubes in the solar convection zone. II. The influence of initial conditions. *Astrophys. J.* **502**, 481. [DOI](#). [ADS](#).
- Cattaneo, F.: 1999, On the origin of magnetic fields in the quiet photosphere. *Astrophys. J. Lett.* **515**, L39. [DOI](#). [ADS](#).
- Fan, Y.: 2009, Magnetic fields in the solar convection zone. *Living Rev. Solar Phys.* **6**, 4.

- Fan, Y., Featherstone, N., Fang, F.: 2013, Three-dimensional MHD simulations of emerging active region flux in a turbulent rotating solar convective envelope: the numerical model and initial results. *ArXiv e-prints*, [arXiv](#).
- Getling, A.V., Buchnev, A.A.: 2010, Some structural features of the convective-velocity field in the solar photosphere. *Astron. Rep.* **54**, 254. [DOI](#). [ADS](#).
- Getling, A.V., Ishikawa, R., Buchnev, A.A.: 2015, Doubts about the crucial role of the rising-tube mechanism in the formation of sunspot groups. *Adv. Space Res.* **55**, 862. [DOI](#). [ADS](#).
- Gurevich, L.E., Lebedinsky, A.I.: 1946, Magnetic field of Sun spots. *J. Phys. USSR* **10**, 337.
- Ichimoto, K., Lites, B., Elmore, D., Suematsu, Y., Tsuneta, S., Katsukawa, Y., Shimizu, T., Shine, R., Tarbell, T., Title, A., Kiyohara, J., Shinoda, K., Card, G., Lecinski, A., Streadner, K., Nakagiri, M., Miyashita, M., Noguchi, M., Hoffmann, C., Cruz, T.: 2008, Polarization calibration of the Solar Optical Telescope onboard *Hinode*. *Solar Phys.* **249**, 233. [DOI](#). [ADS](#).
- Kitchatinov, L.L., Mazur, M.V.: 2000, Stability and equilibrium of emerged magnetic flux. *Solar Phys.* **191**, 325. [DOI](#). [ADS](#).
- Kitiashvili, I.N., Kosovichev, A.G., Mansour, N.N., Wray, A.A.: 2015, Realistic modeling of local dynamo processes on the Sun. *Astrophys. J.* **809**, 84. [DOI](#). [ADS](#).
- Kosovichev, A.G.: 2009, Photospheric and subphotospheric dynamics of emerging magnetic flux. *Space Sci. Rev.* **144**, 175. [DOI](#). [ADS](#).
- Kosovichev, A.G., Stenflo, J.O.: 2008, Tilt of emerging bipolar magnetic regions on the Sun. *Astrophys. J. Lett.* **688**, L115. [DOI](#). [ADS](#).
- Lites, B.W., Akin, D.L., Card, G., Cruz, T., Duncan, D.W., Edwards, C.G., Elmore, D.F., Hoffmann, C., Katsukawa, Y., Katz, N., Kubo, M., Ichimoto, K., Shimizu, T., Shine, R.A., Streadner, K.V., Suematsu, A., Tarbell, T.D., Title, A.M., Tsuneta, S.: 2013, The *Hinode* spectro-polarimeter. *Solar Phys.* **283**, 579. [DOI](#). [ADS](#).
- Lites, B., Casini, R., Garcia, J., Socas-Navarro, H.: 2007, A suite of community tools for spectro-polarimetric analysis. *Mem. Soc. Astron. Ital.* **78**, 148. [ADS](#).
- Luoni, M.L., Démoulin, P., Mandrini, C.H., van Driel-Gesztelyi, L.: 2011, Twisted flux tube emergence evidenced in longitudinal magnetograms: Magnetic tongues. *Solar Phys.* **270**, 45. [DOI](#). [ADS](#).
- Parker, E.N.: 1955, The formation of sunspots from the solar toroidal field. *Astrophys. J.* **121**, 491. [DOI](#). [ADS](#).
- Pevtsov, A., Lamb, J.B.: 2006, Plasma flows in emerging sunspots in pictures. In: Leibacher, J., Stein, R.F., Uitenbroek, H. (eds.) *Solar MHD Theory and Observations: A High Spatial Resolution Perspective*, *ASP Conf. Ser.* **354**, 249. [ADS](#).
- Poisson, M., Mandrini, C.H., Démoulin, P., López Fuentes, M.: 2015, Evidence of twisted flux-tube emergence in active regions. *Solar Phys.* **290**, 727. [DOI](#). [ADS](#).
- Rempel, M., Cheung, M.C.M.: 2014, Numerical simulations of active region scale flux emergence: From spot formation to decay. *Astrophys. J.* **785**, 90. [DOI](#). [ADS](#).
- Shimizu, T., Nagata, S., Tsuneta, S., Tarbell, T., Edwards, C., Shine, R., Hoffmann, C., Thomas, E., Sour, S., Rehse, R., Ito, O., Kashiwagi, Y., Tabata, M., Kodeki, K., Nagase, M., Matsuzaki, K., Kobayashi, K., Ichimoto, K., Suematsu, Y.: 2008, Image stabilization system for *Hinode* (Solar-B) Solar Optical Telescope. *Solar Phys.* **249**, 221. [DOI](#). [ADS](#).
- Stein, R.F., Nordlund, Å.: 2012, On the formation of active regions. *Astrophys. J. Lett.* **753**, L13. [DOI](#). [ADS](#).
- Suematsu, Y., Tsuneta, S., Ichimoto, K., Shimizu, T., Otsubo, M., Katsukawa, Y., Nakagiri, M., Noguchi, M., Tamura, T., Kato, Y., Hara, H., Kubo, M., Mikami, I., Saito, H., Matsushita, T., Kawaguchi, N., Nakajoi, T., Nagae, K., Shimada, S., Takeyama, N., Yamamuro, T.: 2008, The Solar Optical Telescope of Solar-B (*Hinode*): The Optical Telescope Assembly. *Solar Phys.* **249**, 197. [DOI](#). [ADS](#).
- Tsuneta, S., Ichimoto, K., Katsukawa, Y., Nagata, S., Otsubo, M., Shimizu, T., Suematsu, Y., Nakagiri, M., Noguchi, M., Tarbell, T., Title, A., Shine, R., Rosenberg, W., Hoffmann, C., Jurcevic, B., Kushner, G., Levay, M., Lites, B., Elmore, D., Matsushita, T., Kawaguchi, N., Saito, H., Mikami, I., Hill, L.D., Owens, J.K.: 2008, The Solar Optical Telescope for the *Hinode* mission: An overview. *Solar Phys.* **249**, 167. [DOI](#). [ADS](#).
- Tverskoi, B.A.: 1966, A Contribution to the theory of hydromagnetic self-excitation of regular magnetic fields. *Geomagn. Aeron.* **6**, 7.
- Vögler, A., Schüssler, M.: 2007, A solar surface dynamo. *Astron. Astrophys.* **465**, L43. [DOI](#). [ADS](#).
- Warnecke, J., Losada, I.R., Brandenburg, A., Kleorin, N., Rogachevskii, I.: 2013, Bipolar magnetic structures driven by stratified turbulence with a coronal envelope. *Astrophys. J. Lett.* **777**, 2. [ADS](#). [arXiv](#).
- Warnecke, J., Losada, I.R., Brandenburg, A., Kleorin, N., Rogachevskii, I.: 2015, Bipolar region formation in stratified two-layer turbulence. *ArXiv e-prints*, [arXiv](#).